Heat and Mass Transfer (2022) 58:383–394
https://doi.org/10.1007/s00231-021-03072-3

ORIGINAL

Smoke and evacuation modelling of multi-compartment building for nuclear applications

A. M. Bayomy[1] · Q. Chen[1] · K. Podila[1] · L. Sun[1] · T. Beuthe[1]

Received: 11 November 2020 / Accepted: 5 April 2021 / Published online: 24 July 2021

Abstract

Fire events in nuclear power plants represent a significant potential hazard and are an important contributor to the overall operational risks of these facilities. Consequently, a detailed understanding of fire and smoke propagation behaviour in such applications is required for fire performance-based engineering and risk assessment. This paper presents computational fluid dynamics modelling of a postulated fire scenario and occupant evacuation in a typical multi compartment nuclear building. The NIST Fire Dynamic Simulator (FDS) was used to model fire and smoke propagation by adopting large eddy simulation turbulence modelling approach. FDS simulation benchmarking was first performed against available experimental data of a two-storey compartment. Following this, a study was conducted to understand the smoke propagation, distribution of temperature, toxic gas concentrations, and smoke optical density inside a typical multi-compartment nuclear building. The effect of ventilation on the fire and smoke spread was also investigated. Human evacuation modelling was conducted to determine the required evacuation time and toxic gas dose for each occupant. The FDS predicted smoke parameters, including smoke optical density and toxic gas concentrations, were used as inputs to the evacuation modelling. The results suggest that ventilation flows decrease the smoke optical density due to smoke dilution and thereby result in a shorter time for the occupants to evacuate.

Notations

Acronyms

CNL	Canadian nuclear laboratories
CNSC	Canadian nuclear safety commission
FDS	Fire dynamic simulator
FED	Fractional effective dose
FPSA	Fire probabilistic safety analysis
HGL	Hot gas layer
HRR	Heat Release Rate
LES	Large eddy simulation
NPP	Nuclear power plant
NEA	Nuclear energy agency
NIST	National institute of standards and technology
OECD	Organisation for economic c-operation and development
PRISME	Propagation d'un incendie pour des scénarios multi-locaux élémentaires
U.S. NRC	United states nuclear regulatory commission

Symbols

F	Force
v_i	Velocity/speed
m	Mass
CFL	Courant-Friedrichs-Lewy

Greek symbols

τ_i	Relaxation factor

Subscripts

i	Occupant i
j	Occupant j
w	Wall

✉ A. M. Bayomy
ayman.mahmoud@cnl.ca

Q. Chen
qi.chen@cnl.ca

K. Podila
krishna.podila@cnl.ca

L. Sun
lan.sun@cnl.ca

T. Beuthe
thomas.beuthe@cnl.ca

[1] Canadian Nuclear Laboratories, Chalk River, Ontario K0J 1J0, Canada

1 Introduction

Fire hazard analysis (FHA) and fire probabilistic safety analysis (FPSA) have reported that fire accidents are one of the primary contributors to the damage of nuclear power plants (NPPs) [1]. One of the prominent triggers of the ignition have been electrical events [2]. Electrical fires originating in components such as electrical cabinets accounted almost half (~ 46.5%) of all fires in NPPs with other causes such as hot components (16.9%), mechanical origins (7.3%), and self-ignition (5.5%) accounting for the balance. An electrical fire is generally accompanied by the production of smoke and toxic gases, specifically carbon monoxide (CO) that is known to be fatal to the building occupants during a fire event [3]. In addition, during fire, visibility is also impaired due to the release of smoke particles that are released by the fire.

The propagation of fire and smoke has been studied extensively in the past for nuclear and non-nuclear applications. In the case of fires for nuclear applications, past studies have primarily used a single room configuration with a door. Focus areas included, flow behaviour at the doorway [4], influence of the flow area on the progression of the fire [5, 6], and the impact of ventilation [7]. Fire and smoke propagation tests were undertaken for both small- and large-scale multi-room configurations by various international organisations such as the VTT technical research centre in Finland [8] and by others [9, 10].

In addition to the individual studies performed by various leading organisations, collaborative studies were undertaken by the Organisation for Economic Co-operation and Development (OECD) under the Nuclear Energy Agency (NEA) in France. For instance, in the research program PRISME [11], the smoke and heat propagation within five different multi-compartment configurations were studied experimentally. Recently, Pretrel and Vaux, 2019 [12] have also investigated an experimental test of a fire scenario in a two-level geometry with a hole in the ceiling of the lower level. It was found that the fuel burning rate was significantly affected by compartment ventilation. Computational Fluid Dynamics (CFD) modelling was also conducted to complement the experimental study.

CFD modelling of fire and smoke propagation has been widely used in civil applications involving atria, shopping centers, airport terminals, tunnels, transit stations, car parks, and residential apartments [13, 14] However, CFD modelling studies of smoke and fire propagation for multi-compartment buildings related to nuclear applications are limited. Consequently, there is a need to assess existing CFD codes for the prediction of smoke propagation and toxic gas concentrations during fire incidents in nuclear applications [15] Several CFD codes are currently available for fire and smoke modelling. Among these codes, some are fire-specific, such as the NIST Fire Dynamics Simulator (FDS) [16] and OpenFOAM/FireFOAM [17], while others are more generic such as the Siemens STAR-CCM + [18] and ANSYS CFX/FLUENT [19] codes. In addition to the selection of an appropriate CFD code, analyses should account for other factors that present unique challenges, including the timing of fire detection, smoke generation and migration, rate of flame propagation, habitability (including visibility and concentrations of toxic species), and human evacuation time.

The prediction of human evacuation time during a fire accident is one of the most challenging areas of fire protection engineering. According to the Canadian nuclear regulator, the Canadian Nuclear Safety Commission (CNSC), there is a need for further understanding of human performance integrated with fire modelling in an emergency response in nuclear applications [20] Similarly, a task force report by the U.S. NRC [21] concluded that taking human behaviors into consideration in the event of a fire plays an important role in nuclear facility and safety and that egress design should be modelled and analyzed. As a result, evacuation calculations are becoming a part of performance-based analyses and fire modelling to assess the level of safety provided in a building. A comprehensive review of the available evacuation models was undertaken by NIST [22]. Some of the models have been implemented in codes such as Pathfinder [23] and FDS + Evac developed at VTT Technical Research Centre of Finland [24] to study the effect of fire on human evacuation. In addition, Canadian efforts have included the development of a Fire probabilistic risk assessment model based on the CANDU Fire Database [25] to quantitatively evaluate plant damage states and core damage frequencies related to fire events.

The main objective of the present study is to develop capabilities at Canadian Nuclear Laboratories (CNL) that can be used to predict the smoke propagation and required human evacuation time in a non-vented and ventilated multi-compartment building in nuclear applications. The predictive capabilities for the progression of the smoke largely depend on the ability to correctly capture unsteady turbulence characteristics associated with fire and smoke propagation. In this study, the NIST Fire Dynamics Simulator (FDS) was used to perform CFD modelling of a representative fire scenario in a typical multi-compartment building in an NPP by adopting a Large Eddy Simulation (LES) turbulence modelling approach. LES models have been widely used for fire and smoke modelling applications since they are capable of predicting transient turbulent flow phenomena [26]. A computational evacuation model (FDS + Evac [24]) was used to predict the required evacuation time of occupants by considering human-fire interaction, decision making processes, and the interaction with other individuals.

Since experiments for the fire scenarios in nuclear applications are limited, the benchmarking of FDS was undertaken using experiments of a two-room compartment by Pretrel and Vaux [12] Subsequently, FDS was used to predict the effect of smoke propagation on the distributions of temperature, optical density, and CO concentration at different locations inside a new multi-compartment NPP building geometry. Ventilation effects were also considered, along with the human-fire interactions to estimate the evacuation time required for safe evacuation. Other known factors such as detection time and relaxation factor of the occupants were also examined.

2 Benchmarking FDS simulation using pretrel and vaux, 2019 [12] data

A test condition (test ID# PR2_VSP_4 from Table 2 in Pretrel and Vaux, 2019 [12]) was simulated with FDS to assess the simulation capabilities of the code. The representative geometry (Fig. 1) was developed in FDS using the experimental specifications. The model was subject to measured fuel mass loss rate of the Heptane pool as an input to capture the fire growth heat release rate (HRR) as a function of time. As used in experiments, upper room air supply and exhaust flow rate were set at 1366 m^3/h and 2373 m^3/h, respectively, while the air supply to the lower room was set at 948 m^3/h.

Available experimental measurements at two locations were used to perform an assessment of the FDS predictions. These two locations were marked as CC and SW in the lower and upper rooms as presented in Fig. 1. Overall, FDS predictions captured the experimental trends of the temperature variation with the room height acceptably shown in Fig. 2a. Furthermore, in the lower room, the gas temperature was higher near the ceiling than at the floor due to accumulation of smoke in the vicinity of the hole at the ceiling of the lower room. While the movement of the smoke propagation from the lower room (fire room) to the upper room through the ceiling hole, a sudden decrease in the smoke temperature was presented at location CC due to its movement from a hotter region to a colder region. It was observed that the discrepancy for temperature as a function of room height at location CC and SW was higher in the lower room compared to the upper room. It should be noted that, Pretrel and Vaux have not reported the random uncertainty in the measurements. Furthermore, the instrument (a SARTORIUS weighing balance) used by investigators to measure the fuel burning rate was reported to produce lower values than the actual burning rate [12]. This may have resulted in the use of a lower burning rate as input to the simulation which may in turn have resulted in the lower predicted gas temperature observed in the current simulations against the measured temperature. In addition, the temporal variation of the temperature was under-predicted (Fig. 2b) in the lower room at the SW location (at 1.05 m and 2.05 m respectively). Based on the

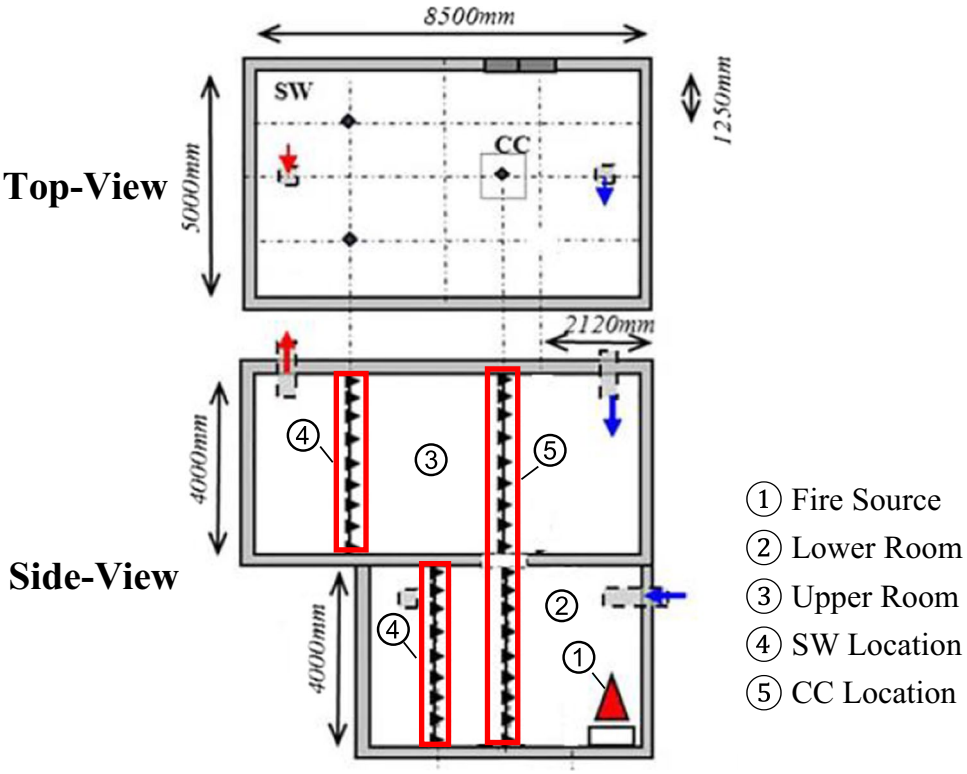

Fig. 1 Experimental facility used by Pretrel and Vaux, 2019 [12]

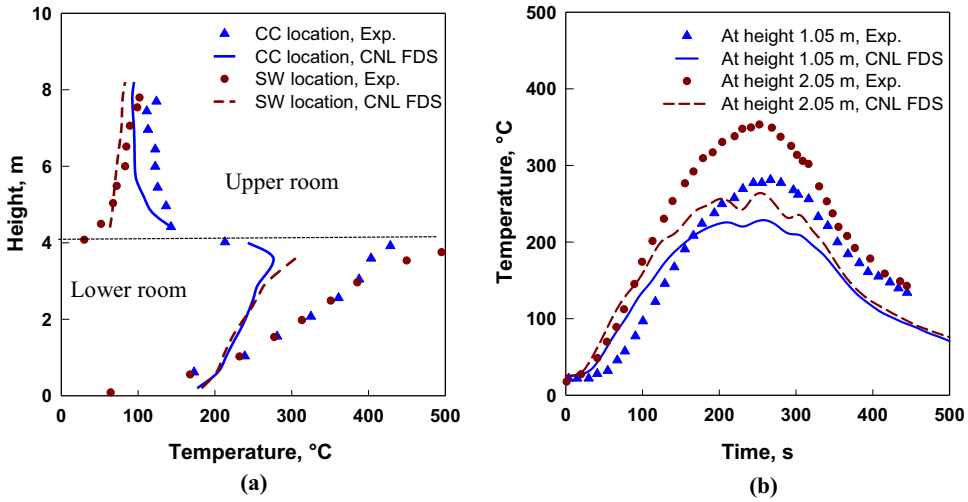

Fig. 2 Temperature variations; (**a**) with the room height, (**b**) with time

limited benchmarking undertaken here, the methodology was able to qualitatively predict the experimental trends. Consequently, the approach adopted for the benchmarking was further extended to model fire and smoke propagation in the multi-compartment building of a different configuration including three rooms in the upper level.

3 FDS model for two-storey multi-room compartment building

3.1 Development of the computational domain

The computational domain for the simulation of a multi-compartment building was generated based on the DIVE facility used by the PRISME fire research program [11]. The primary difference between the present study geometry and DIVE facility was the location of the room labelled basement in Fig. 3. In the DIVE facility, a single room was located at the top, whereas in the current study, this top room was moved to the basement as a fire room. The computational model for the current study was built in FDS using the dimensions listed in Table 1.

In the current model, the basement room was connected to room A by a square ceiling hole (with dimensions of 0.2 m×0.2 m), while all upper rooms and the corridor were connected to each other by doors. All walls were made of 0.3 m thick reinforced concrete and were equipped with one inlet and one exhaust duct (0.2 m×0.2 m) that forms the ventilation network. The total supply/exhaust flow rate of the air was set at 3400 m^3/h. Since ventilation is a limiting parameter that affects fire and smoke propagation behaviour, both non-vented and ventilated fire scenarios were examined in this study.

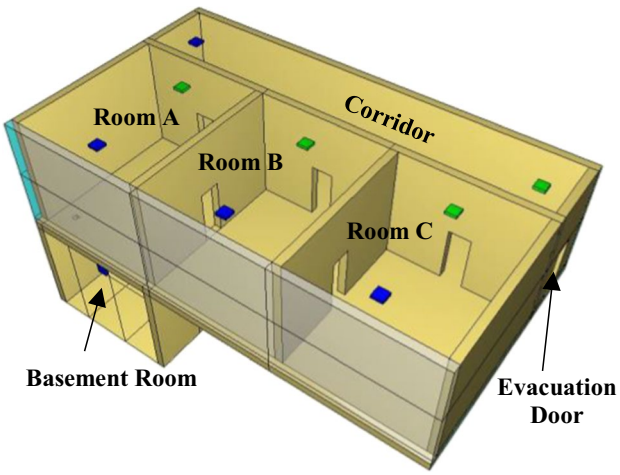

Fig. 3 FDS computational domain

3.2 Description of the fire pool

A fire scenario due to electrical malfunction in bundles of qualified XPE/neoprene cables inside an isolated aluminum control cabinet was simulated as the fire origin (Fig. 4a). The HRR used in this study and the phases associated with the progression of the fire are presented in Fig. 4b.

3.3 Methodology

The conservation equations of mass, momentum, and energy were solved using a finite difference method in FDS. An LES turbulence model implemented in FDS

Table 1 Geometry compartment dimensions

Geometry	Dimensions (L×W×H) (m)
Basement	6×8.5×4
Room A	6×5×4
Room B	6×5×4
Room C	6×5×4
Corridor	15×2.5×4
Fire Cabinet	1.2×0.6×2

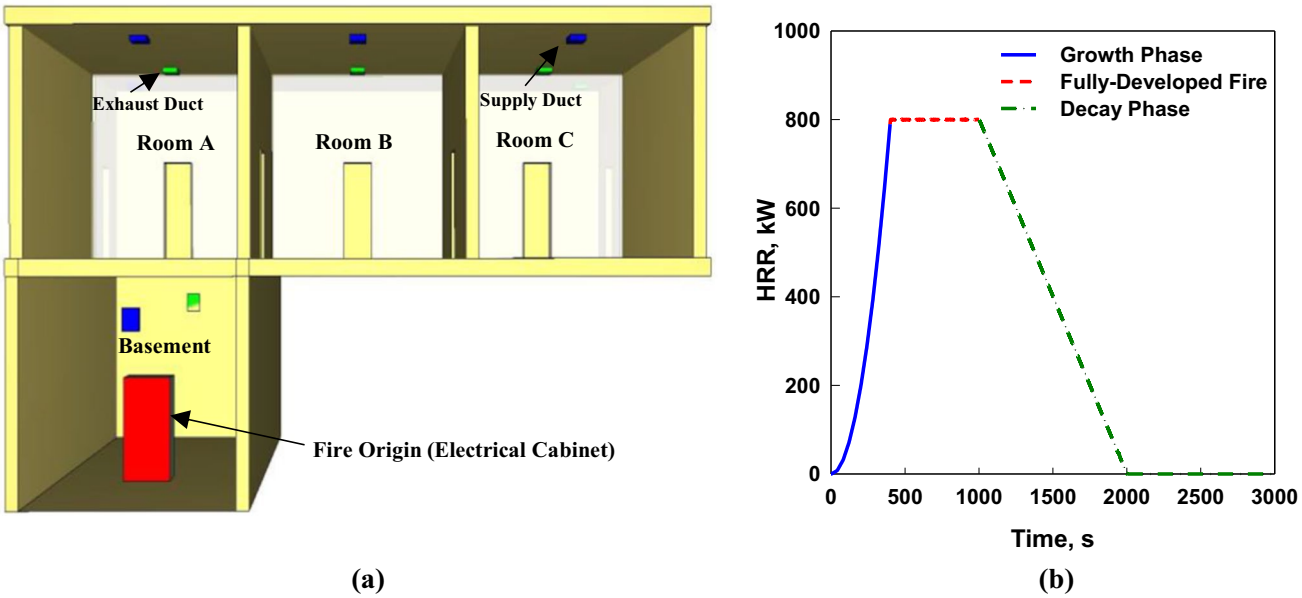

Fig. 4 Fire pool description; (**a**) fire origin, (**b**) HRR used as an input to the FDS model

version 6.7.1 was used for the current simulations. The code used source terms and boundary conditions that described the turbulent combustion of fuel, thermal radiation, soot-laden gases, thermal properties of real materials, the presence of sprinklers and smoke detectors, and a variety of other features that influence fire in the buildings. The convergence of the solution was checked for errors in mass conservation, flow reversal over the time step, and the magnitude of change in the velocity solution. An explicit predictor–corrector scheme with second order discretization accuracy in space and time was used for solving the equations. The flow obstructions were simulated using a simple immersed-boundary method in the computational domain [27].

The Smagorinsky eddy viscosity sub-grid closure was applied in the LES model to resolve the turbulent shear flow of smoke and fire propagation [27]. A value of 0.2 was used for the Smagorinsky coefficient, and the turbulent Prandtl and Schmidt numbers were set to the recommended values of 0.5 in FDS. Constant values of CO and soot yields were used in the present study to initialise the mixture fraction-based combustion model; defined as;

$$y_{CO} = \frac{mass\ of\ Co\ in\ products}{mass\ of\ fuel\ reacted} \tag{1}$$

$$y_{soot} = \frac{mass\ of\ soot\ in\ products}{mass\ of\ fuel\ reacted} \tag{2}$$

where, y_{CO} and y_{soot} represent the initial CO and soot yields. A fast reaction assumption was made in the mixture model that resulted in a state relation between the oxygen mass fraction and mixture fraction. Once the mixture fraction was calculated by LES at each location, the species concentration of oxygen, fuel, and other products as a function of mixture fraction were evaluated.

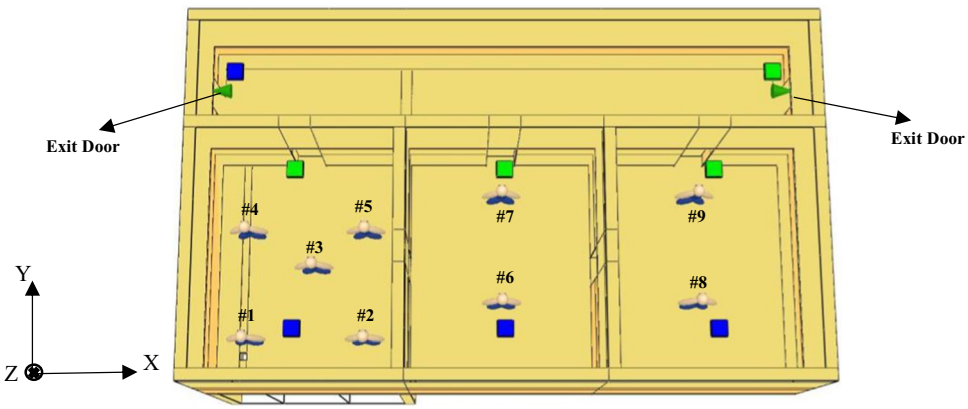

Fig. 5 Occupants locations in upper rooms (top view)

Table 2 Occupant positions

Person #	1	2	3	4	5	6	7	8	9
Horizontal direction (X, m)	1.2	4.4	3	1.2	4.4	8.1	8.1	13.4	13.4
Vertical direction (Y, m)	1.4	1.4	3.3	4.3	4.3	2.3	5.2	2.3	5.2

The computational time was set to 3000 s to allow the fire to reach the decay phase presented in Fig. 4b. During the simulation, the time step was dynamically adjusted according to local velocities ($dt < \min(\frac{\Delta x}{u}, \frac{\Delta y}{v}, \frac{\Delta z}{w})$). The convergence criteria of the solution was verified at every time step in terms of the magnitude change in the Courant-Friedrichs-Lewy (CFL) condition [28].

The value for the initial oxygen concentration was set for the combustion model to capture all the phases of fire evolution in the HRR curve. This value varies case-by-case, but for the present study 0.207 mol/mol initial oxygen concentration was used. This ensured that the fire propagation within the computational domain did not halt (extinguish) as a result of depletion of oxygen.

3.4 Evacuation modelling

Evacuation modelling during an accidental scenario can be treated by adopting either an agent-, or flow-based approach. Within this study, an agent-based approach that is capable of handling dense crowds was adopted. An evacuation algorithm can be divided into two main aspects; the occupant movement and the interaction between occupants and fire field.

In an occupant movement algorithm [29], each occupant is represented in form of three circles combined in a two-dimensional plane. Each occupant has a defined mass and moves towards the exit door with a preferred walking velocity vector field, v_i^0 where the vector field is obtained using the FDS flow solver. In addition, an equation of motion that comprises of a combination of forces on occupants, (e.g. such as interaction forces among occupants and interaction forces between the occupants and building walls) was used in the evacuation modelling by FDS to resolve the movement of each occupant, formulated as follows:

$$F_i = \underbrace{\frac{m_i}{\tau_i}\left(v_i^0 - v_i\right)}_{(A)} + \underbrace{F_{ij} + F_{iw}}_{(B)} \tag{3}$$

The movement of each occupant towards the evacuation door is influenced by the relaxation factor (τ_i) that affects the magnitude of the momentum term (A) in Eq. 3. FDS default parameters were used in this study to evaluate the interaction forces [30, 31] represented by term (B) in Eq. 1. A similar equation was also considered within this study to resolve the interaction torques among the occupants.

The interaction between occupants and fire field is an important aspect in evacuation modelling. The habitability criteria of the building depends on the smoke concentration (e.g. smoke optical density) and toxic gas concentration to which occupants would be exposed [6]. The evacuation algorithm within the FDS + Evac code [24] utilises the predicted smoke optical density for the determination of the visibility towards exit doors along each occupant trajectory. During a fire event, smoke reduces occupant walking speed due to the reduction in visibility according to an experimentally based correlation [32]. The occupant speed is modelled to decrease to a minimum value of 0.1 m/s, following which occupants continue to move at this speed until they are incapacitated by the toxic effects of the fire products [24].

Within the Evac code used here, the toxic effects of combustion products were treated using Purser's Fractional Effective Dose (FED) concept [33]. The FED methodology accounts for the toxic effect of carbon monoxide and other combustion products, a carbon dioxide induced hyperventilation factor, and hypoxia due to depletion of oxygen on each of the occupants in a domain. An occupant is considered incapacitated when the FED reaches the threshold value of unity.

In the present study, the evacuation was simulated for a total of nine occupants located in the upper level of the multi-compartment geometry as presented in Fig. 5. The detailed location of each occupant is provided in Table 2.

4 Grid refinement analysis

Grid cell topology and mesh density affect the solution accuracy of a numerical model. Hence, in this study, sensitivity to mesh partition and cell sizes were examined to determine an optimum combination of quick computational time and an acceptable numerical accuracy. Since the source of the

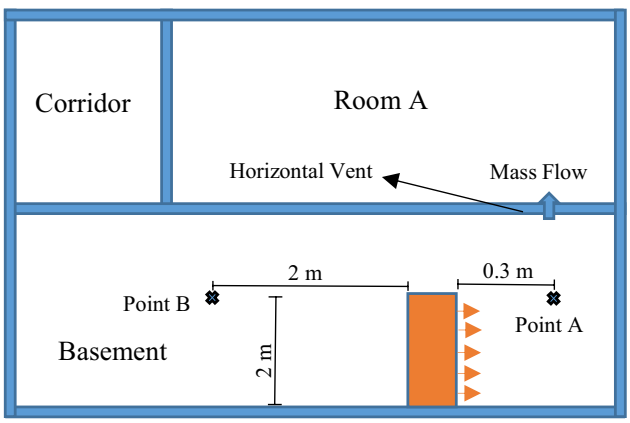

Fig. 6 Mesh sensitivity points locations

Table 3 Mesh zones sensitivity analysis

Case #	Mesh Configuration		Maximum Gas Temperature (°C)	
1 (reference case)	single mesh for all computational domain		Point A	Point B
			662.94	259.87
	Basement Mesh Zones	Total Number of Mesh Zones		
2	one mesh	5	651.73	257.75
3	3 meshes	7	666.02	258.23
4	9 meshes	13	675.33	263.03

fire in the present multi-compartment domain was located in the basement, the sensitivity analyses were limited only to the basement. Details pertaining to mesh partition and cell size were evaluated using default model constants. The simulations were executed in a parallel mode using the in-house CNL computational cluster MINERVA. The data analyses for the sensitivity studies were undertaken at two locations in the basement; near (~0.3 m: point A) and further (~2 m: point B) away from the source of the fire (aluminium cabinet) as shown in Fig. 6.

4.1 Sensitivity to mesh partitions in the basement

In order to reduce the computational time, a parallel computation approach was used. To implement this strategy, the computational domain was divided into a number of mesh zones. Unfortunately, it was found that the choice of domain partition could result in solution inconsistencies at the mesh boundaries. To minimize the solution inconsistency/variation due to mesh partition, a mesh zone sensitivity analysis was conducted based on three mesh partition schemes in the basement (identified as case #2, 3 and 4), while one mesh zone was used for each room on the upper floor was used as described in Table 3. The solution using only one mesh for the entire computational domain served as a reference case (case #1) to determine the effect of mesh partition on the solution accuracy and the computational run time.

Table 4 Details of the basement mesh sensitivity refinement

Case #	Basement mesh count	Basement avg. cell size (m)	(D/Δx) (-)
4 (base case)	26,320	0.2	4.4
5	92.120	0.13	6.8
6	316,120	0.09	10.1
7	618,520	0.07	12.6

The maximum gas temperatures at point A and B were compared among the four cases. It was found that the maximum reduction in the computational time was achieved by case #4 (4.5 h) compared with the reference case (23.6 h). Furthermore, numerical solution accuracy in case #4 was within the acceptable range of 2% compared to the reference case. Therefore, the mesh partition applied in case #4 (i.e. nine mesh zones in basement) was selected in the following study.

4.2 Sensitivity to mesh size

Since the size of a grid cell (Δx) greatly influences the accuracy of the LES approach, a grid sensitivity analysis was also performed to ensure the final results are independent of mesh count used in the model. In this study, the ratio between the fire characteristic diameter (D) to grid size (Δx) was maintained at ~ 10. This value lies within the recommended range of 5–10 specified in a previous study [34]. In order to accurately capture the details of fire growth and propagation, a local mesh refinement (see Fig. 7) was conducted in the fire region in the basement room where the model is the most sensitive to smoke movement and dynamics, while the mesh in the other regions was not refined. The mesh refinement ratio between consecutive meshes was maintained at 1.3 as recommended in Celik et al., 2008 [35].

Using the mesh configurations listed in the Table 4, the predicted gas temperature at point A is evaluated in Fig. 8. It was observed that the predicted trends for the transient evolution of temperatures were similar, however, the peak values at the fully developed phase (Fig. 4a)

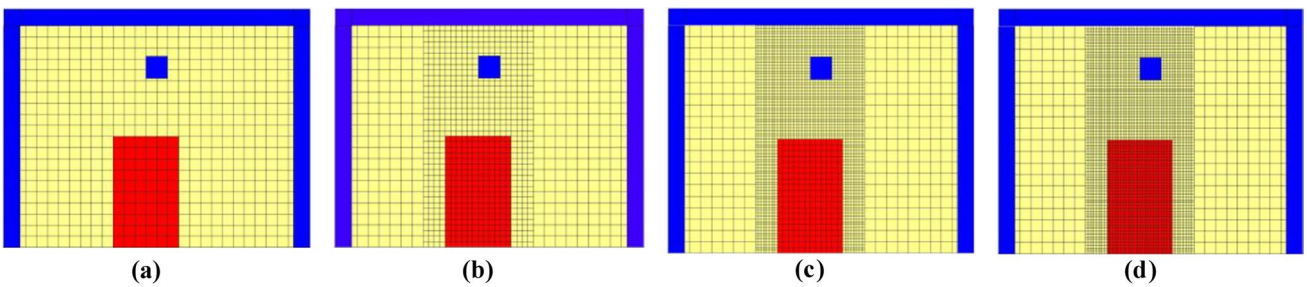

Fig. 7 Meshes used in the basement during refinement process

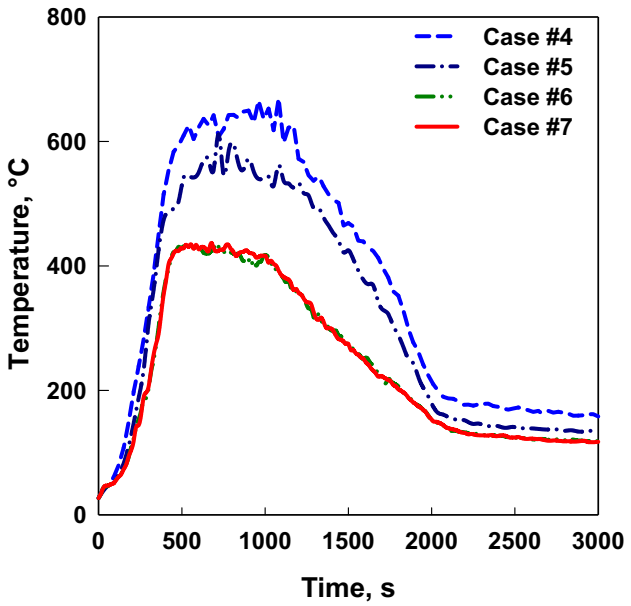

Fig. 8 Effect of grid refinement on prediction of gas temperature at point A

were significantly different except for the cases #6 and 7. Therefore, mesh configuration of case 6 was used for all subsequent simulations.

5 Results and Discussions

5.1 Fire and smoke parameter for non-vented condition

As illustrated in Fig. 9, the smoke started to exhaust from the side of the cabinet at 50 s (Fig. 9a), and gradually accumulated under the basement ceiling. A small portion of smoke spread through the ceiling hole to room A while the smoke layer thickness was increasing in the basement room at 100 s (Fig. 9b). Smoke completely filled room A, B, and the corridor at 400 s (Fig. 9c) and the entire building at 600 s (Fig. 9d). As seen in Figs. 8a and b, the hot gases rose as a ceiling jet and entrained the cold air in room A, thereby resulting in lower gas temperatures in the vicinity of the plume.

As presented in Fig. 10a, the gas temperature at the center of basement room (fire room) increased gradually during the fire growth phase (up to 400 s), then stabilized around 220 °C until 1600 s, and decreased to ~ 100 °C at 3000 s. This trend corresponded closely to the HRR used in the study shown in Fig. 4b. The gas temperatures in the upper level rooms and the corridor were lower compared to that of basement and varied from 30 °C to 60 °C. Optical smoke density, which represents a critical parameter to determine the building habitability during a fire event was found to be higher in the basement compared to the upper level, thereby implying lower visibility that can have detrimental effects on egress during a fire incident. It was found that the optical density value reached at maximum of 180 m^{-1} at the center of the basement room due to smoke accumulation under the ceiling (see Fig. 10b).

The ceiling jet phenomenon observed in Fig. 9a impacted the variation of the HGL (hot gas layer) in the basement. As seen in Fig. 11, the temperature peaked initially at the onset of the ceiling jet and gradually decreased with the progression of time. The current methodology predicted the temperature of the HGL under the basement ceiling (see Fig. 11) to increase to around 250 °C during the fully developed phase of the fire, then decrease to 115 °C during the fire decay phase.

The HGL height (see Fig. 11) started at 4 m (basement room height) and decreased rapidly while the smoke layer thickness was gradually increasing under the ceiling during the fire growth phase. The HGL height stabilized at ~ 0.5 m during the fully developed and decay phases of the fire. Similar behaviour was seen for room A.

5.2 Effect of forced ventilation

To study the effects of ventilation on the fire propagation, a fire scenario was simulated that included mechanical ventilation with a total supply/exhaust flow rate of 3400 m^3/h (the rate required to cause ~ 5 complete room air changes per hour).

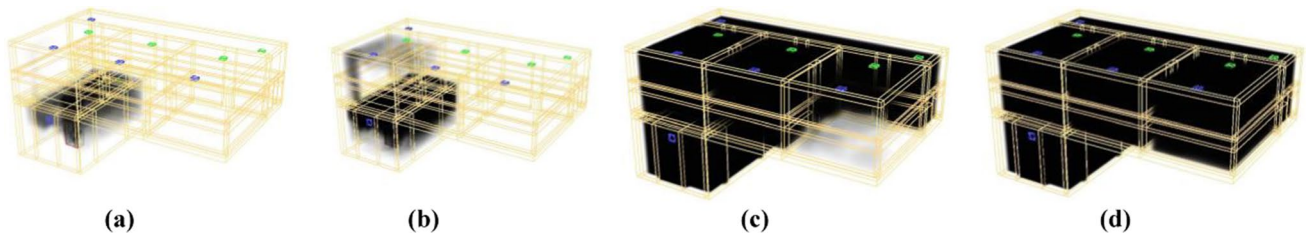

Fig. 9 Smoke temporal propagation in non-vented fire scenario

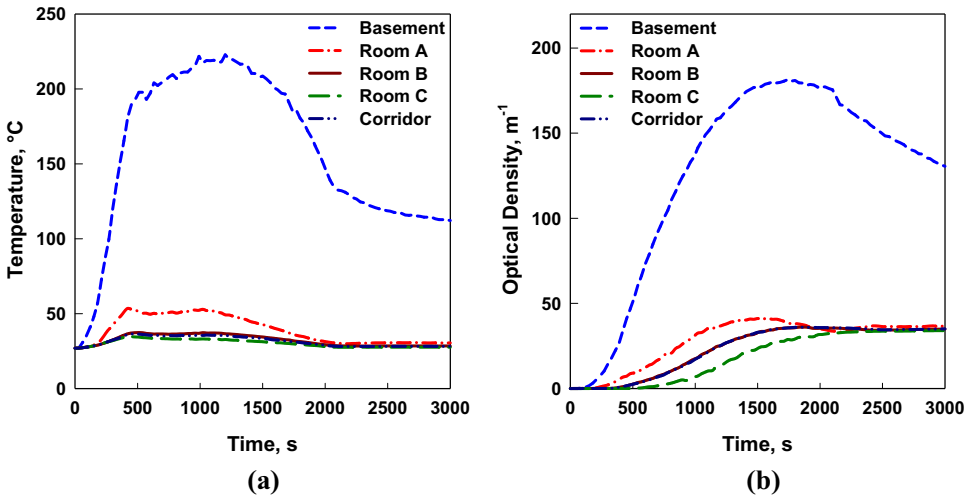

Fig. 10 Smoke parameters at center of each room; (**a**) gas temperature, and (**b**) optical density

It was observed that the gas temperature near the fire was slightly lower in the presence of ventilation due to the mixing of cold ventilation air with the hot combustion gases. It was noted that the gas temperature in the fire room reached close to 400 °C under ventilated condition, same observation was made in OECD PRISME experiments [11]. However, the effect of the ventilation was more dominant on other parameters such as optical density, CO concentration, and pressure as shown in next figures.

The hot gas mass flow rate to room A through the ceiling hole increased significantly under ventilated conditions as shown in Fig. 12. This finding matches the previous observation that ventilation flow promotes the propagation of hot gases.

Under ventilated condition, the optical smoke density peak in the basement was much lower in comparison with the non-vented condition (Fig. 13) since the smoke was diluted by the ventilation flow. Unlike in the non-vented condition, smoke in the basement was completely removed by ventilation exhaust ducts during the fire decay phase. A similar phenomenon was also observed in room A (Fig. 13).

As shown in Fig. 14a, the oxygen concentration in the basement room decreased gradually while the fire was growing and consuming oxygen. During the decay phase of the fire, the oxygen concentration slightly increased due to a decrease in oxygen consumption. The oxygen concentration was reduced by ~ 50% in the non-vented condition, and by only ~ 20% in the ventilated condition due to the air ventilation flow.

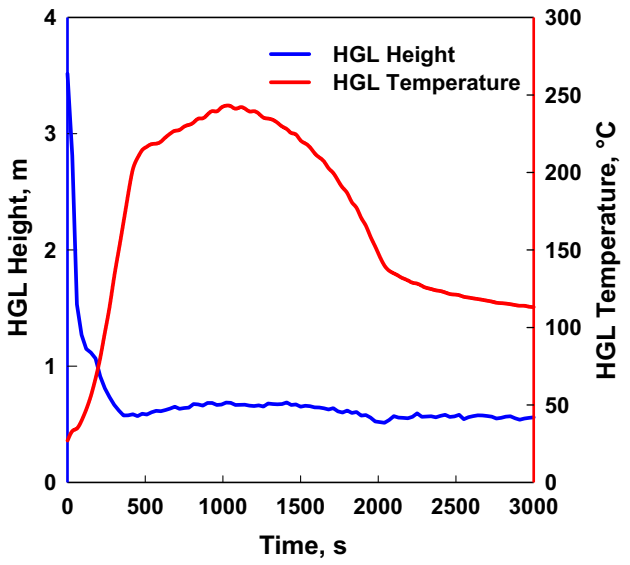

Fig. 11 HGL height and temperature at the center the basement

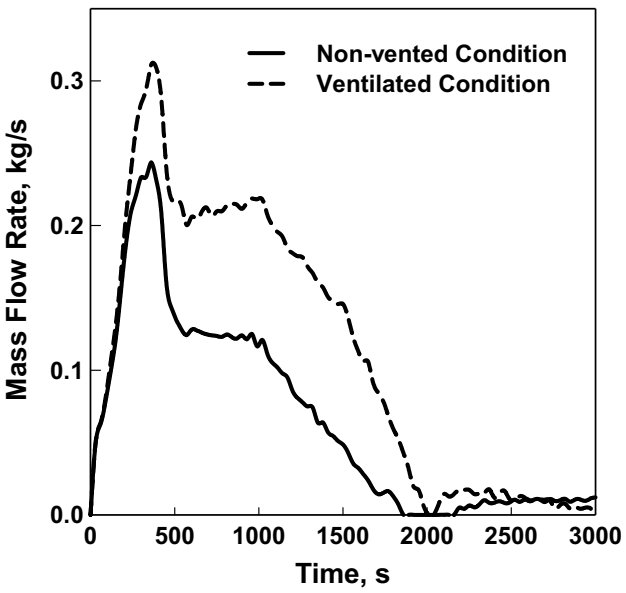

Fig. 12 Ventilation effect on ceiling hole mass flow rate

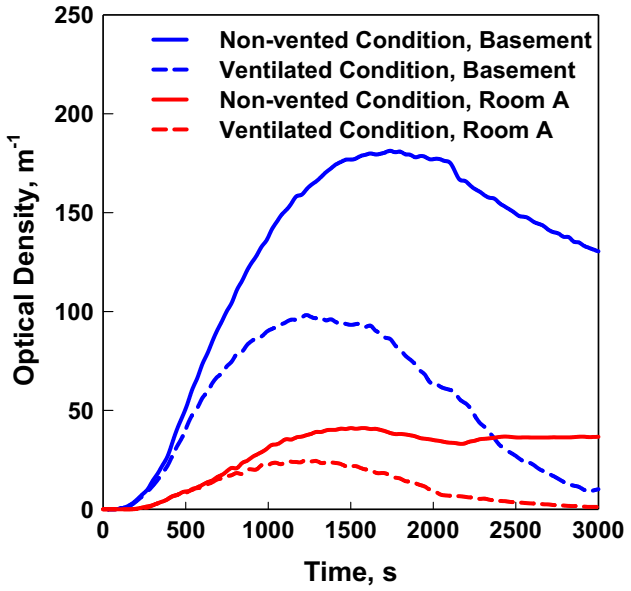

Fig. 13 Effect of the ventilation on smoke optical density

PRISME fire tests [11] demonstrated the importance of pressure variations in the overall prediction of fire scenarios in both non-vented and ventilated compartments. As seen in Fig. 14b, the pressure in the ventilated condition was much higher than that of the non-vented condition since the cold air supply causes a decrease in smoke temperature and an increase in smoke volume. Under these conditions, the pressure increased gradually during the fire growth and fully developed phases due to exhausted hot gases and combustion products from the fire. Once the fire HRR reduced to zero (no smoke production) at 2000s, the pressure stabilized.

5.3 Human evacuation

Fire detection time (also called reaction time), at which the occupants start to evacuate from the building, is an important parameter that affects the evacuation time and varies based on building geometry and fire location. As reported by Lan et al., 2020 [6], smoke optical density represents the critical parameter that can be used to estimate the fire detection time. When the optical density exceeds the threshold value of 0.3 m^{-1} the occupants start to evacuate the building. Consequently, the predicted optical smoke density at each occupant initial location was used to determine the occupant detection time (Fig. 15) under both non-vented and ventilated conditions. Since smoke optical density reached the threshold value of 0.3 m^{-1} at 180 s for both non-vented and ventilated conditions, the fire detection time for all occupants was set at 180 s.

It was noted that the required evacuation time for nine occupants was shorter under the ventilated condition (22 s) than that for the non-vented condition (25 s) (Fig. 16a). Under normal ventilated conditions, lower optical density due to smoke dilution by ventilation air flow (as noted in Fig. 13) led to a higher visibility, and, as a result, a faster evacuation of occupants.

As seen in Fig. 16a occupants exited the region of the fire in a step-wise manner. Furthermore, the FED was significantly higher in the non-vented condition than that experienced under the ventilated condition (Fig. 16b). However, maximum accumulated FED values were much lower than the threshold value of unity which means all occupants could evacuate safely from the building without excessive exposure to toxic gases.

6 Conclusions

Fire and smoke modelling along with occupant evacuation modelling have been performed using the NIST Fire Dynamic Simulator and Evac codes to assess the habitability of a typical multi-compartment building in an NPP in the event of a postulated electrical cabinet fire. The key findings of the present work are summarised as follow:

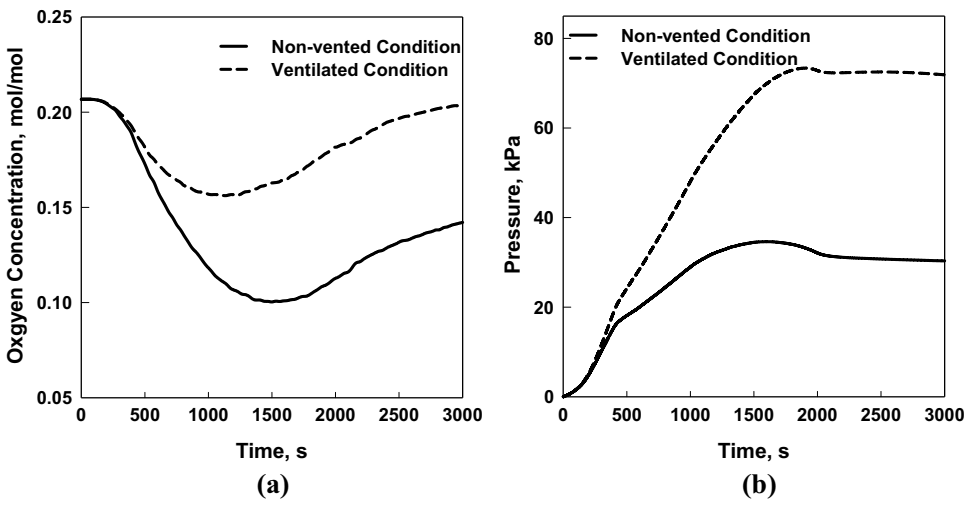

Fig. 14 Ventilation effect on; (**a**) oxygen concentration in the basement, and (**b**) pressure variation throughout the building

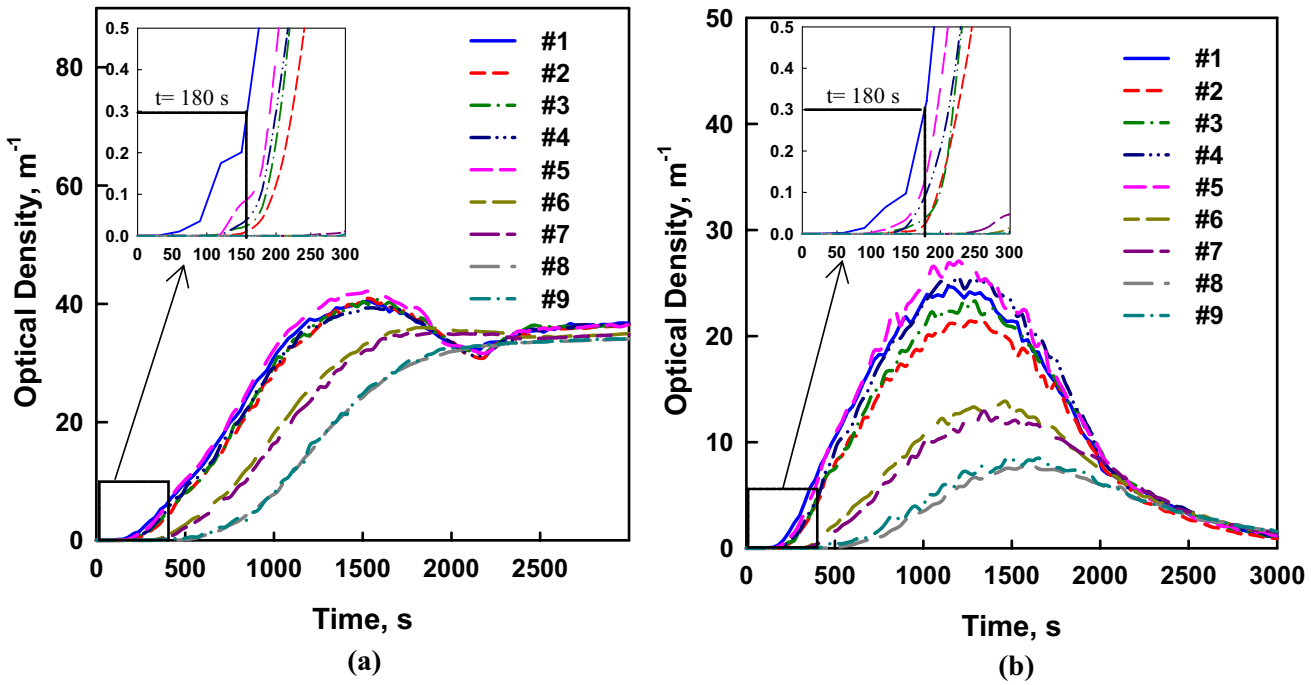

Fig. 15 Optical density at occupant locations (see Table 2); (**a**) non-vented condition, and (**b**) ventilated condition

- Fire and smoke modelling benchmarking was performed against previous experimental data.
- During the benchmarking, FDS was able to qualitatively predict the experimental trends.
- Temperatures were predicted to increase rapidly throughout the growth and fully developed phases of the fire and stabilized with the progression of the time.
- Mechanical ventilation reduced smoke optical density by 46% in the basement and 38% in room A compared to non-vented condition due to smoke dilution by ventilation air flow.
- The oxygen concentration was reduced by only ~ 20% in the ventilated condition due to the air ventilation flow.
- Mechanical ventilation doubled the average building pressure during the fire event since the cold air supply causes a decrease in smoke temperature and an increase in smoke volume.
- Evacuation modelling predicted that the required evacuation time for nine occupants was 25 s for non-vented condition and 22 s for ventilated condition.

FDS simulation results will be further assessed and benchmarked with available experimental data as a future work of the current study.

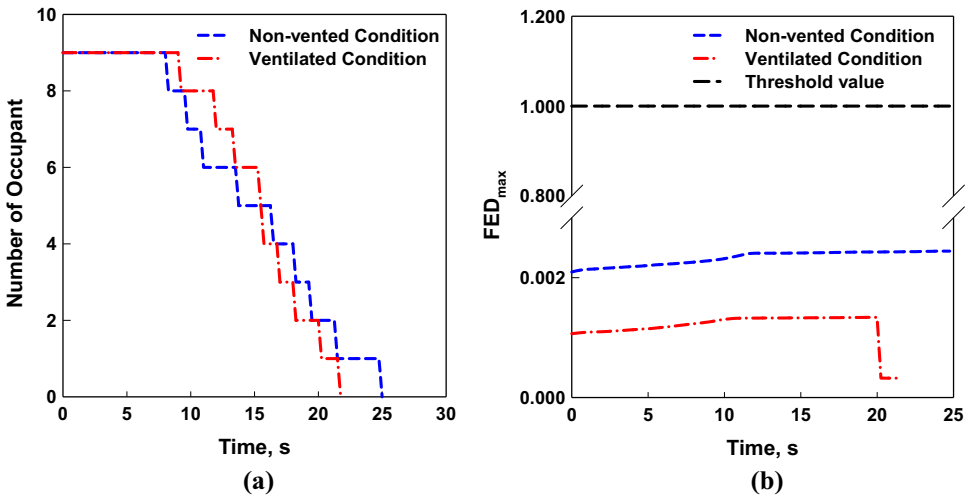

Fig. 16 Occupant evacuation parameters; (**a**) evacuation time, and (**b**) fractional effective dose (FED)

Funding This study has been funded by Atomic Energy of Canada Limited, under the auspices of the Federal Nuclear Science and Technology Program.

Code availability Not Applicable.

Declarations

Conflict of interest: Not Applicable.

References

1. OECD Report (2000) Fire risk analysis, fire simulation. Fire Spreading and Impact of Smoke and Heat on Instrumentation Electronics. State of the Art Report, NEA/CSNI/R, vol (99)27
2. Werner W, Angner A, Röwekamp M, Gauvain J (2009) The OECD fire database. 11th International Post Conference on Fire Safety in Nuclear Power Plants and Installations
3. Babrauskas V, Gann RG, Levin BC, Pabo M, Harris RH, Peacock RD, Yasa S (1998) A methodology for obtaining and using toxic potency data for fire hazard analysis. Fire Safe J 31:345–358
4. Zukoski E, Kubota T (1985) Experimental study of environment and heat transfer in a room fire, mixing in doorway flows and entrainment in fires plumes. NIST Report NPS-GCR-85–493
5. Parkes AR, Fleischmann CM (2005) The impact of location and ventilation on pool fire in a compartment. Fire Safety Science Proceedings of the Eighth International Symposium, pp. 1289–1300
6. Sun L, Podila K, Chen Q, Bayomy AM, Rao YF (2020) Computational fluid dynamics modeling of fire and human evacuation for nuclear applications. J Nucl Eng Radiat Sci 6(1):011112. https://doi.org/10.1115/1.4044531
7. Hagglund B, Werling P, Bengtson S (1988) An experimental study of the smoke spread in a two plane compartment. In Proceedings of the third Asia-Oceania symposium on Fire Science and Technology, International Association for Fire Safety Science
8. Vaari J, Hietaniemi J (2000) Smoke ventilation in operational fire fighting. Part 2. Multi-storey Buildings. VTT Report419, Espoo. Report 419. 951-38-5580-5
9. Matsuyama K, Mizuno M, Wakamatsu T (2001) A systematic experiments of room and corridor smoke filling for use in calibration of zone and CFD fire models for engineering fire safety design of buildings. Fire Sci Tech 21(1):43–55
10. Rutherford L (2002) Experimental results for pre-flash over fire experiments in two adjacent ISO compartments research project report, University of Canterbury, New Zealand
11. Audouin L, Rigollet L, Prétrel H, Le Saux W, Röwekamp M (2013) OECD PRISME project: Fires in confined and ventilated nuclear-type multi-compartments - Overview and main experimental results. Fire Saf J 62:80–101
12. Pretrel H, Vaux S (2019) Experimental and numerical analysis of fire scenarios involving two mechanically ventilated compartments connected together with a horizontal vent. Fire Mater 43(5):514–529
13. Hadjisophocleous GV, Lougheed GD, Cao S (1999) Numerical study of the effectiveness of atrium smoke exhaust systems. ASHRAE Trans 105:699
14. Kang K (2007) Application of Code Approach for Emergency Evacuation in a Rail Station. Fire Technol 43(4):331–346
15. Emmons HW, Tanaka T, DiNenno PJ (2008) The SFPE Handbook of Fire protection Engineering4th edition. National Fire Protection Association, Quincy, MA 02269, pp. 2–37(2–53)
16. VTT and NIST (2013) "Fire Dynamics Simulator, User's Guide", NIST Special Publication 1019, 6th edn. National Institute of Standards and Technology, Gaithersburg, MA
17. OpenFOAM Version 1712 Documentation, https://www.openfoam.com/documentation/cpp-guide/html/index.html (Last accessed on May 7, 2018).
18. STAR CCM+ Version 13.02 User Guide, 2018
19. ANSYS CFX/FLUENT, Version 19.0, Documentation, 2017
20. Elder P (2018) Opportunities for Canadian Nuclear Laboratories in Support of Nuclear Safety and Regulation. Presentation at Canadian Nuclear Laboratories' CNL Federal Lab Day. Ottawa, ON, February 15, 2018
21. U.S. NRC and SNL (2008) A Phenomena Identification and Ranking Table (PIRT) Exercise for Nuclear Power Plant Fire Modeling Applications. NUREG/CR-6978, November 2008
22. NIST (2010) A Review of Building Evacuation Models, 2nd edition. Technical Note 1680, November 2010
23. Pathfinder User Manual (2018) Thunderhead Engineering, 403 Poyntz Avenue, Suite B Manhattan, KS 66502, U.S.A
24. Korhonen T (2018) Fire Dynamics Simulator with Evacuation: FDS+Evac, Technical Reference and User's Guide. VTT Technical Research Center of Finland, FDS 6.6.0, Evac 2.5.2, DRAFT, February 2018
25. Shalabi H, Hadjisophocleous G (2018) CANDU Fire Probabilistic Risk Assessment (PRA) Model. CNL Nuclear Review, Available online 18 Dec. 2018
26. Zhang W (2002) Turbulence statistics in a fire room model by large eddy simulation. Fire Saf J 37:721–752
27. VTT and NIST (2013) Fire Dynamics Simulator, Technical Reference Guide, Volume 1: Mathematical Model. NIST Special Publication 1018 6th Ed., National Institute of Standards and Technology, Gaithersburg, MA, November, 2013
28. McGrattan KB (2002) Fire Dynamics Simulator (FDS) Manual. Technical Reference Guide
29. Werner T, Helbing D (2003) The social force pedestrian model applied to real life scenarios. In Pedestrian and Evacuation Dynamics-Proceedings of the Second International Conference. University of Greenwich, London, p 17–26
30. Korhonen T, Hostikka S, Heliovaara S, Ehtamo H (2007) FDS+Evac: Modelling social interactions in fire evacuation. In Proceedings of 7th International Conference on Performance-Based Codes and Fire Safety Design Methods, pp. 241–250. Society of Fire Protection Engineers, Boston, MA
31. Helbing D, Farkas I, Molnár P, Vicsek T (2002) Simulating of Pedestrian Crowds in Normal and Evacuation Situations. Pedestrian and Evacuation Dynamics, Schreckenberg, M. and Sharma, S.D. (eds.), Springer, Berlin, pp. 21–58
32. Nilsson D, Johansson M, Frantzich H (2009) Evacuation experiment in a road tunnel: A study of human behaviour and technical installations. Fire Saf J 44(4):458–468
33. Purser DA (2003) Toxicity Assessment of Combustion Products. In SFPE Handbook of Fire Protection Engineering. 3rd ed., pp. 2–83–2–171, National Fire Protection Association, Quincy, MA
34. U.S. NRC and EPRI (2005) EPRI/NRC-RES Fire PRA Methodology for Nuclear Power Facilities. vol. 1 and 2, NUREG/CR-6850 (EPRI 1011989)
35. Celik IB, Ghia U, Roache PJ, Freitas CJ, Coleman H, Raad PE (2008) Procedure for Estimation and Reporting of Uncertainty due to Discretization in CFD Applications. Journal of Fluids Engineering, vol. 130